IRANIAN JOURNAL OF CATALYSIS

Efficient Epoxidation of Alkenes using New Organometallic Catalysts ((E)-2,6-dimethoxy-4-((2-(5-methyl-1,3,4-thiadiazol-2-yl)hydrazono)methyl)phenol M: Cr, Fe, Co, Cu): An Antimicrobial and Theoretical Study of Catalyst

Rasha Shaker Mahmood[a]*; Mohammed Ismail Abowd[b]; Asmaa Badr Sabti[a]

a) Department of Chemistry, College of Science, University of Misan, Maysan, Iraq

b) Department of Chemistry, College of Science, University of Thi-Qar, Thi-Qar, Iraq

Received 13 May 2023; received in revised form 15 July 2023; accepted 23 July 2023 (**DOI: 10.30495/IJC.2023.1986079.2007**)

ABSTRACT

In this research, a novel approach for the epoxidation of alkene derivatives was constructed. Based on this fact, the appropriate ligand was provided from the reaction of hydrazine hydrate and 5-methyl-1,3,4-thiadiazole-2-thiol. Then, after preparation of the intermediate compound, the treatment of the pointed compound and 4-hydroxy-3,5-dimethoxybenzaldehyde in the presence of a few drops of glacial acetic acid for 3h was done in order to a final ligand. Then, the synthesized ligand was metallated using Cr, Fe, Co, and Cu to obtain a series of organometallic catalysts. The synthesized organometallic catalysts were analyzed using CHNS analysis, FT-IR spectroscopy, and magnetic susceptibility. Then, the organometallic complexes containing (Chromium, Iron, Cobalt, and Copper) are applied in the epoxidation of various alkenes to provide corresponding target products and provide moderate to good yields. The prepared organometallic complexes were investigated relative to the reusability and loss of metal into the medium of the reaction. In addition, the optimized chemical structures of organometallic complexes were investigated using DFT calculation.

***Keywords**: Epoxidation, alkene, organometallic, catalyst, antimicrobial, DFT calculation*

1. Introduction

Schiff base ligands (Imine) are simply synthesized and produced into metal complexes involving all metal ions [1]. Some of the Schiff base complexes exhibit excellent catalytic activity in different organic reactions. In general, Schiff base ligands are provided using the condensation reaction of amine derivatives, especially primary amines, and aldehydes. The resultant products share in binding with metal ions through nitrogen lone pair electrons [2]. It is notable that the Schiff base ligands with ketones are produced less readily than with aldehydes [3]. Based on the binding environments of metal ions, the mono-, di-, and tri-, as well as multi-dentate chelating of Schiff base, are designed [4]. Schiff base complexes, including metal ions (Organometallic catalysts), are efficient and robust catalysts in heterogeneous and homogeneous organic reactions. Among them, organometallic catalysts, especially the transition metal Schiff base complex, are well-known and obvious catalysts for the oxidation of different organic compounds using various oxidation agents [5-12]. The last two decades have seen a rise in interest in the varied applications of Schiff base catalysts, which include chelating carrying nitrogen and oxygen donor atoms, in the domains of catalysis and organic transformations in both academia and industry [13-23]. As we may know, epoxides are efficient and important intermediate substrates in organic transformations [24-28]. **Scheme 1** exhibits different catalysts and conditions for the oxidation of styrene. The organometallic catalysts, especially Schiff base containing metal ions, are known as powerful organometallic catalysts for the epoxidation of alkenes using different oxidation agents such as oxygen,

*Corresponding author:
E-mail address: *rasha_shaker@uomisan.edu.iq* (**R. S. Mahmood**);

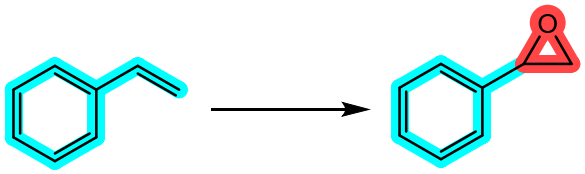

Scheme 1. Different methodology for oxidation of styrene: A) SnO_2@2D-graphitic carbon nitride, room temperature, O_2, Yield: 98.1% [32]. B) $Pd_4Cu_8L_8$ cage, Room temperature, $NaIO_4$, Yield: 89.3% [33]. C) Nanoscale CuO, TBHP as oxidation agent, more than 95% conversion, 6h, 6 runs reusability [34]. D) Schiff base condensation of *p*-terphenyl-4,4″-dialdehyde and 3-aminopropyl-trimethoxysilane containing Ag nanoparticles, CO_2 as mild oxidation, 24 h, 86% [35]. E) Cu/Co-Co PBA-250, 99% conversion of styrene, 6 h [36]. F) GF-CoS_2/CoS heterostructures anchored on graphite felt and bromine, 3.5 h, Yield: 97% [37]. G) Br^-/Br_2, acid and heat-modified graphite felt (AHGF) electrodes, 95% conversion, 6 h [38]. H) MnO_x nanocatalysts with abundant oxygen vacancies, 90.0% selectivity towards styrene oxide, and a turnover frequency of 581 h^{-1} [39].

hydrogen peroxide, Sodium hypochlorite, Sodium periodate, Iodosobenzene, and Potassium peroxymonosulfate, as single atom oxygen donors [29-31]. However, metal inactivation and leaching to the reaction medium have been shown to reduce the applicability of these organometallic complexes. Based on the importance of the oxidation of alkenes, we designed a series of novel organometallic catalysts containing Cr, Fe, Co, and Cu for high epoxidation of alkenes using oxidation agent s such as $NaIO_4$.

2. Experimental

2.1. General

Without additional purification, we purchased all of our ingredients, solvents, and reagents from Fluka, Sigma-aldrich, BDH, and Merck. Capillary tube melting point measurements using an Electro thermal IA9000 instrument were used to acquire the uncorrected melting points of the produced complexes and ligands. Shimadzu model (Kyoto, Japan) spectrophotometer was used to record FT-IR spectra on a KBr disk in the range of 400-4000 cm^{-1}, and thin-layer chromatography (TLC) was performed on silica gel (60) F254 Merck. Euro EA3000 elemental analyzer (Carlo Erba, Milan, Italy) was used for the CHNS analysis's measuring. Using tetramethylsilane (TMS) as a standard, ^{1}H-NMR and ^{13}C-NMR spectra were acquired using an Inova model Ultra shield 500MHz spectrometer. Solvent DMSO-d6 was employed, and the chemical shift was denoted in parts per million (δ=ppm).

2.2. Preparation of Ligand

A mixture of (99%) hydrazine hydrate (0.1 mol, 4.85mL), 5-methyl-1,3,4-thiadiazole-2-thiol (**1**) (0.1 mol, 13.2 g) in 50 mL of ethanol was heated for 10 h. The reaction was followed by TLC. Then, the overplus solvent was decanted off, and the mixture was filtered, and a dark yellow solid was remained from C_2H_5OH. m.p: 162-164 °C, yield=98% compound (**2**). After preparation of compound (**2**), 0.02 mol, (2.6 g) of compound (**2**) and 4-hydroxy-3,5-dimethoxybenzaldehyde (**3**) (0.02 mol, 3.64 g) was heated in 20 mL of absolute ethanol in the presence of few drops of glacial acetic acid for 3h. The reaction was monitored by TLC. At the end of the reaction, the reaction mixture was made cold to ambient temperature. The dark yellow solid result was filtered off and washed with water, and recrystallized from C_2H_5OH. m.p: (d>180) °C, yield 95%.

2.3. Preparation of organometallic complexes

The organometallic catalysts were synthesized by the mixing (0.001 mol) of a ligand with (0.001 mol) of the different metal salts including ($CrCl_3.6H_2O$, $FeCl_3.6H_2O$, $CoCl_2.6H_2O$, and $CuCl_2.2H_2O$) in 15mL absolute ethanol for 2h. Then, the precipitate was filtered and washed many times with C_2H_5OH or (H_2O:C_2H_5OH) to remove remained salts or ligand; then the precipitated catalysts were dried.

2.4. Typical Approach for the Epoxidation of Alkenes using organometallic catalysts

In a 25 mL round-bottom flask equipped with a magnet and condenser, a mixture of alkene (2.0 mmol), $NaIO_4$ (2.0 mmol), and complexes (I-IV) (240 mg) in 5 mL of water: ethanol (2:1) was heated. The monitoring of the reaction was performed using GC. After the end of the reaction, the organometallic catalysts were filtered and washed using $CHCl_3$ and CH_2Cl_2 (3×5 mL). The resultant compound was refined on a (SiO_2) silica-gel plate or column chromatography to receive the pure compound.

3. Results and Discussion

Scheme 2 exhibits the general approach for the epoxidation of alkenes by sodium periodate using the synthesized organometallic catalysts (I-IV). The synthesized organometallic complexes were identified using FT-IR spectroscopy, Mass spectroscopy, melting point, magnetic momentum, and CHN analyzer.

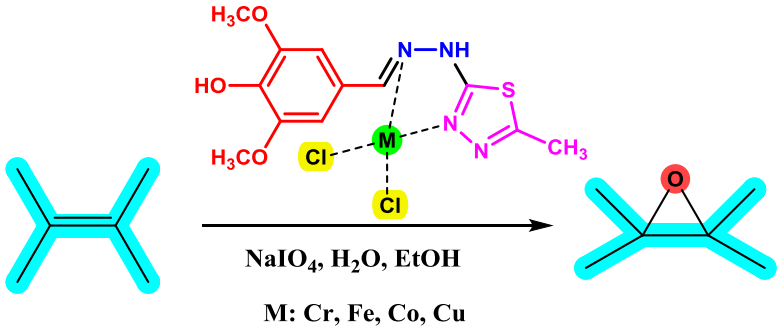

Scheme 2. Epoxidation of alkenes using $NaIO_4$

Initially, the desired ligand was synthesized from the reaction of hydrazine hydrate and 5-methyl-1,3,4-thiadiazole-2-thiol (**1**) in 50 mL of ethanol 10 h under reflux conditions. Then 0.02 mol of compound (**2**) and 4-hydroxy-3,5-dimethoxybenzaldehyde (**3**) was heated in 20 mL of absolute ethanol in the presence of acetic acid for 3h. The dark yellow solid result (Ligand) was filtered off and washed with water and recrystallized from C_2H_5OH. (**Scheme 3**). The structure of the ligand was identified and approved using FT-IR spectroscopy, ^{1}H NMR, ^{13}C NMR, mass spectroscopy, and CHNS analyzer.

The ^{1}H NMR Spectrum of the ligand in DMSO-d_6 peak assignments is characterized by the presence of signal at δ (1H, 12.85) ppm due to (NH) protons near to the ring of thiadiazole, δ (1H, 10.19) ppm due to (O-H) phenolic proton, azomethine group (N=CH) appeared signal at δ (1H, 8.44) ppm, signal at δ (2H, 7.15) ppm belong to aromatic protons, (O-CH_3) protons seemed at δ (6H, 3.92) ppm, while a peak at δ (3H, 2.65) ppm due to the proton of methyl group near to the ring of thiadiazole. All of the peaks are shown in **Fig. 1**.

The ^{13}C NMR Spectrum of the ligand peaks assignments of chemical shifts are characterized by the peak at δ (19.00) ppm due to the carbon of methyl group, chemical shifts for (OCH_3) methoxy group appeared at δ (56.6) ppm, peak associated to δ (N = C) of azomethine group that appeared at δ (156.40) ppm. In addition, the aromatic carbon rings appeared at a range δ (118. -122) ppm. The spectrum performs peaks at lower fields at δ (192) ppm due to the carbon of the ring near to (NH) group. All of the peaks are shown in **Fig. 2**.

The mass spectrum of the ligand exhibited (**Fig. 3**) a peak $[M]^{+\cdot}$at 294 m/z, which is in adaptation with the molecular formula $[C_{12}H_{14}N_4O_3S]^+$. Other signals are due to the subsequent fragments such as $[C_{12}H_{14}N_4O_2S]^+$=278m/z, $[C_{11}H_{11}N_4O_2S]^+$=263m/z, $[C_{11}H_{12}N_4OS]^+$=248m/z, $[C_{10}H_{10}N_4S]^+$=218m/z, $[C_9H_{12}NO_3]^+$=182m/z, $[C_6H_8N_4S]^+$=168m/z base peak, $[C_8H_{10}O_3]^+$=154m/z, $[C_2HN_4S]^+$=113m/z.

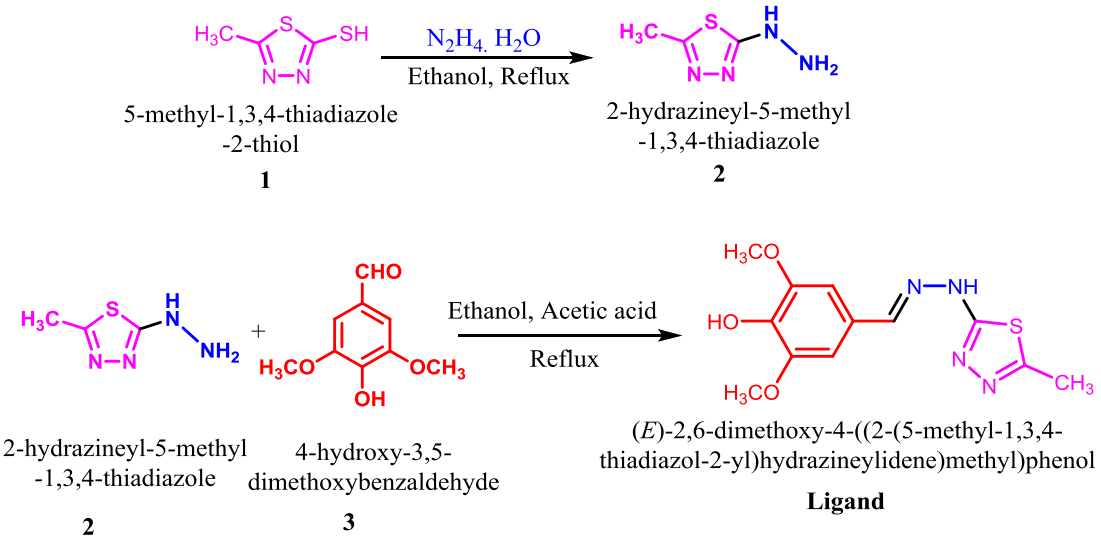

Scheme 3. Synthesis of novel ligand for production of an organometallic catalyst

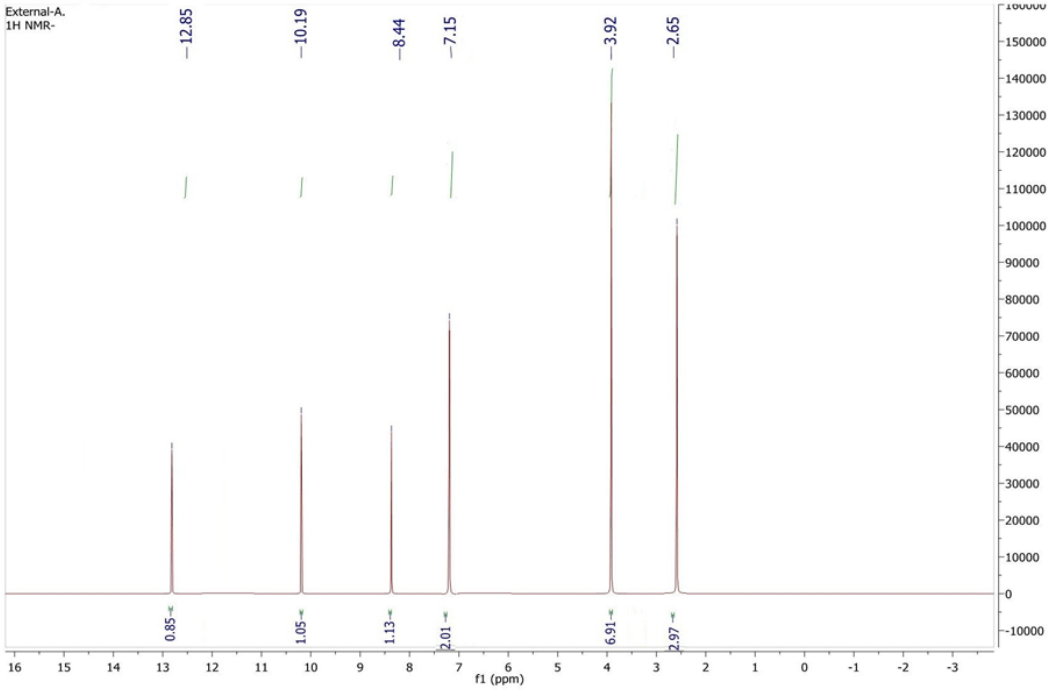

Fig. 1. ^{1}H NMR spectra of synthesized ligand

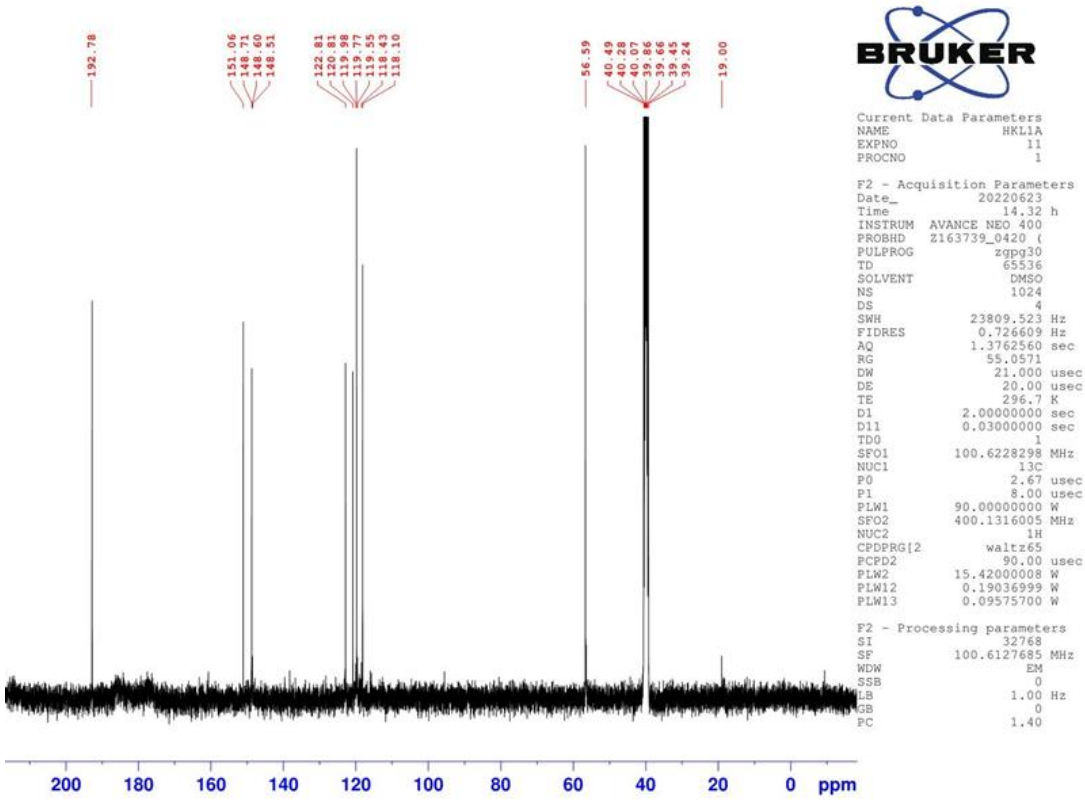

Fig. 2. ^{13}C NMR spectra of synthesized ligand

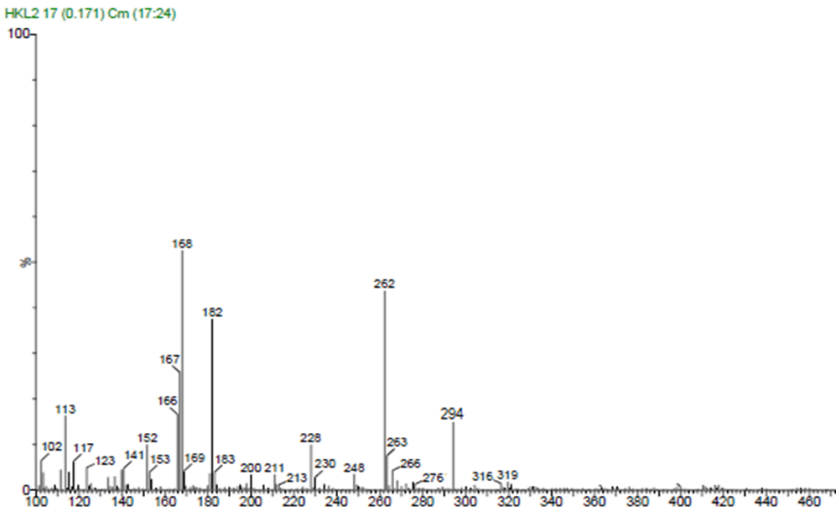

Fig. 3. Mass spectrum of synthesized ligand

After the preparation of the ligand, the organometallic catalyst containing Cr, Fe, Co, and Cu were produced as following: The mixture of ligand and (0.001 mol) of the different metal salts including ($CrCl_3.6H_2O$, $FeCl_3.6H_2O$, $CoCl_2.6H_2O$, and $CuCl_2.2H_2O$) in 15 mL absolute ethanol for 2 h was heated. Then, the precipitate was smoothed down and washed many times with C_2H_5OH or (H_2O: C_2H_5OH) to eliminate unreacted salts or ligand, then precipitated catalyst was dried. The Chemical structure of the organometallic complexes is shown in **Fig. 4**. In addition, the physical, magnetic moment, molar quality in DMF, and elemental analysis of synthesized ligand and metallic complexes are shown in **Table 1**. The magnetic momentum of each metal complex was measured. These magnetic measurements give a good idea about the electronic state of the transition metal ion of these complexes. The measured magnetic momentum amount of the Chromium (III) complex was 3.7 BM and 2.9 BM for Fe (III) complex; therefor it is expected octahedral geometry. The magnetic momentum amount was 4.5 BM for Co (II) complex, which is expected for tetrahedral geometry. The magnetic momentum amount of Cu (II) was 1.76 BM so that suggesting square planar geometry Cu (II). These amount are agreeing with the theoretical calculation of hyperchem by using the PM3 method.

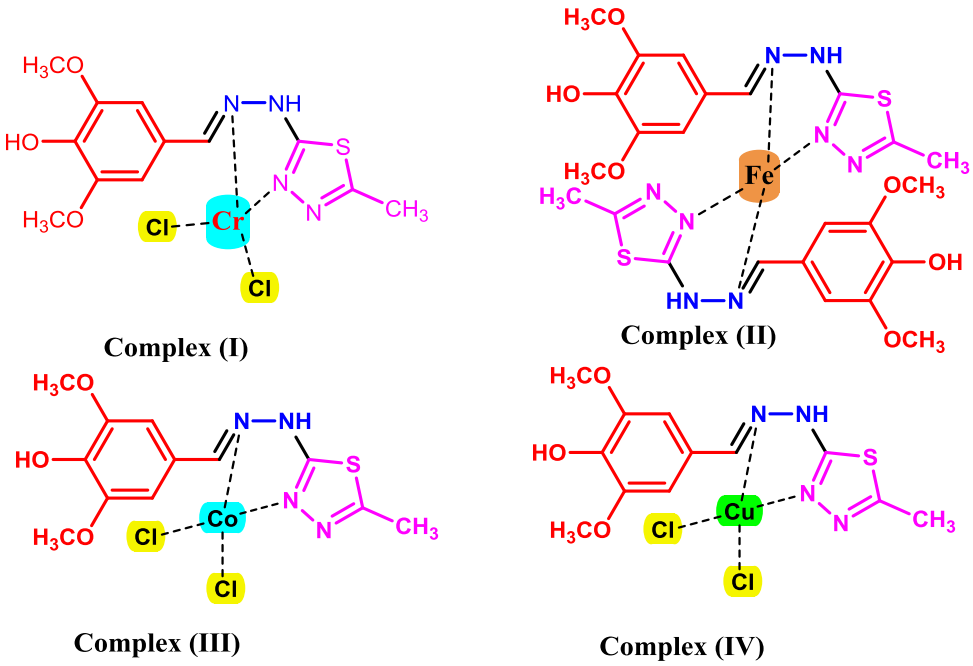

Fig. 4. The chemical structure of the synthesized organometallic catalyst.

Table 1. Physical, magnetic moment, molar quality in DMF, and elemental analysis of synthesized ligand and metallic complexes

Complex/Ligand	M. P. (°C)	Color	CHN Analyzed			Λ $Scm^2.mol^{-1}$	μeff B.M
			Carbon	Hydrogen	Nitrogen		
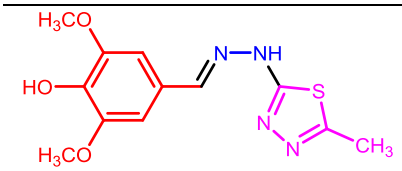	d[a]>170	yellow	20.12 Exp. 19.04 Cal.	3.93 Exp.4.79 Cal.	48.35 Exp. 48.97 Cal.	-	-
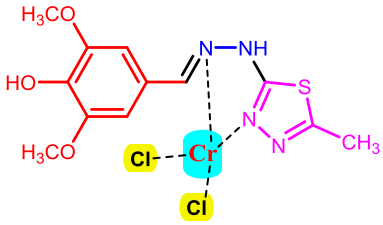	d>300	green	N. D.[b]	N. D.	N. D.	24.3	3.8
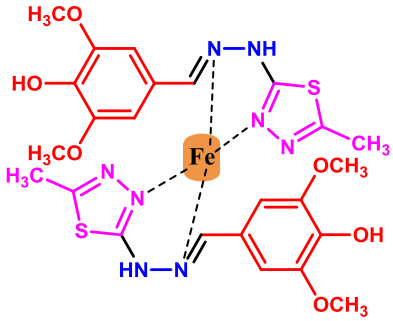	d>219	brown	N. D.	N. D.	N. D.	38.6	2.3
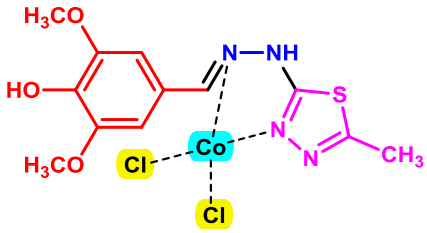	d>292	dark grey	N. D.	N. D.	N. D.	14.65	4.7
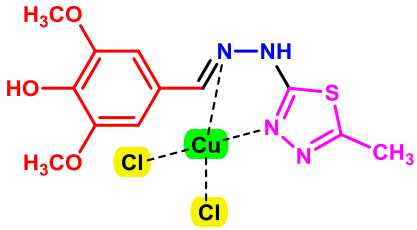	d>265	green yellow	N. D.	N. D.	N. D.	12.7	1.7

d: Decompose, N.D.: Not Done

The FT-IR spectra of the ligand and organometallic complexes were recorded using the KBr disc for the ligand and CsI for the complexes (**Table 2**) (**Fig. 5**). The infrared spectrum of the ligand exhibited stretching vibration bonds at the following frequencies (cm^{-1}) and their identical assignments at ν (O-H 3300), ν (NH 3254), ν (C=N 1660 imine and 1519 ring), ν (C-S-C 1357 asymm., 1292 symm.) [40, 41]. The ligand binds the nitrogen of azomethine with the metal ion to make a stable chelate ring. The stretching vibration of the complexes demonstrates the shift of azomethine groups (ν C = N) [42] to the lower or higher frequencies, as shown in **Table 2**. This is due to the coordination of the metal ion with the ligand. The spectra of complexes demonstrated new band vibrational modes for the M-N and M-Cl group frequencies as a result of bonding the metal ion with the ligand. This indicates that the coordination occurred through the (N) and (Cl) atoms.

Table 2. FT.IR spectral data of the ligand and their metal complexes

Complex/Ligand	Metal−N	Structure Movement	C-S-C (sym.)	C-S-C (Asym.)	C=N ring	C=C	C=N imine	NH	O-H
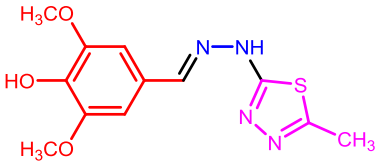	-	1024	1292	1357	1519	1608	1660	3254	3300
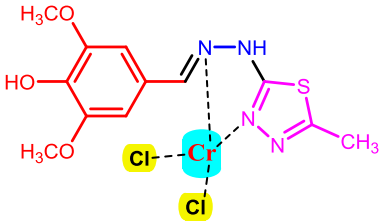	451	1026	1292	1358	1520	1608	1659	3255	3301
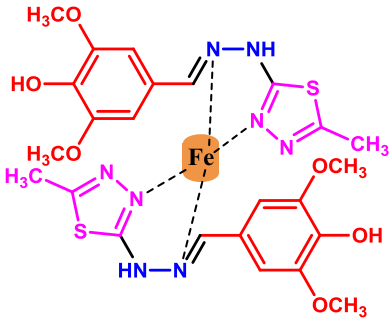	460	1029	1283	1355	1517	1606	1661	3190	3299
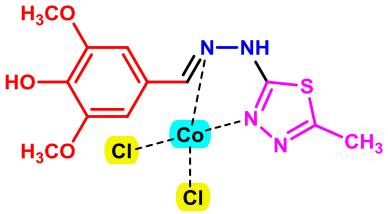	453	1022	1291	1356	1519	1608	1660	3186	3298
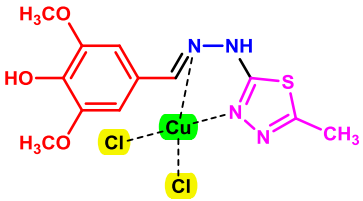	454	1024	1290	1356	1519	1609	1660	3188	3299

The mass spectra of synthesized organometallic catalysts are shown in **Fig. 6**. The mass spectrum of the complex $[Cr(L)Cl_3]$ showed a molecular ion peak $[M]^{+\cdot}$ (470) m/z, which is equivalent to the molecular mass of the complex. This complex showed another fragment ion peak with loss of aqua and three chlorine atoms at m/z (452,417,381,346) due to $[Cr(L)Cl_3]^+$, $[Cr(L)Cl_2]^+$, $[Cr(L)Cl]^+$ and $[Cr(L)]$, respectively (**Fig. 6a**).The mass spectrum of the complex $[Fe(L)_2Cl_2]Cl$ showed a molecular ion peak $[M]^{+\cdot}$ (750) m/z which is equivalent to the molecular mass of the complex. This complex showed another fragment ion peak with loss of three chlorine atoms at m/z (714,679, 644) due to $[Fe(L)_2Cl_2]^+$, $[Fe(L)_2Cl]^+$ and $[Fe(L)_2]^+$, respectively (**Fig. 6b**). The mass spectrum of the complex $[Co(L)Cl_2]$ showed a molecular ion peak $[M]^{+\cdot}$at 424 m/z, which is equivalent to the molecular mass of the complex. This complex showed fragment ion peaks with loss of two chlorine atoms at (389 m/z and 353) m/z due to $[Co(L)Cl]^+$ and $[Co(L)]^+$ respectively (**Fig. 6c**). The mass spectrum of the complex $[Cu(L)Cl_2]$ showed a molecular ion peak $[M]^{+\cdot}$ at (431) m/z, which is equivalent to the molecular mass of the complex. This complex showed fragment ion peaks with loss of chlorine atoms at m/z (393, 357) due to $[Cu(L)Cl]^+$ and $[Cu(L)]^+$ respectively (**Fig. 6d**).

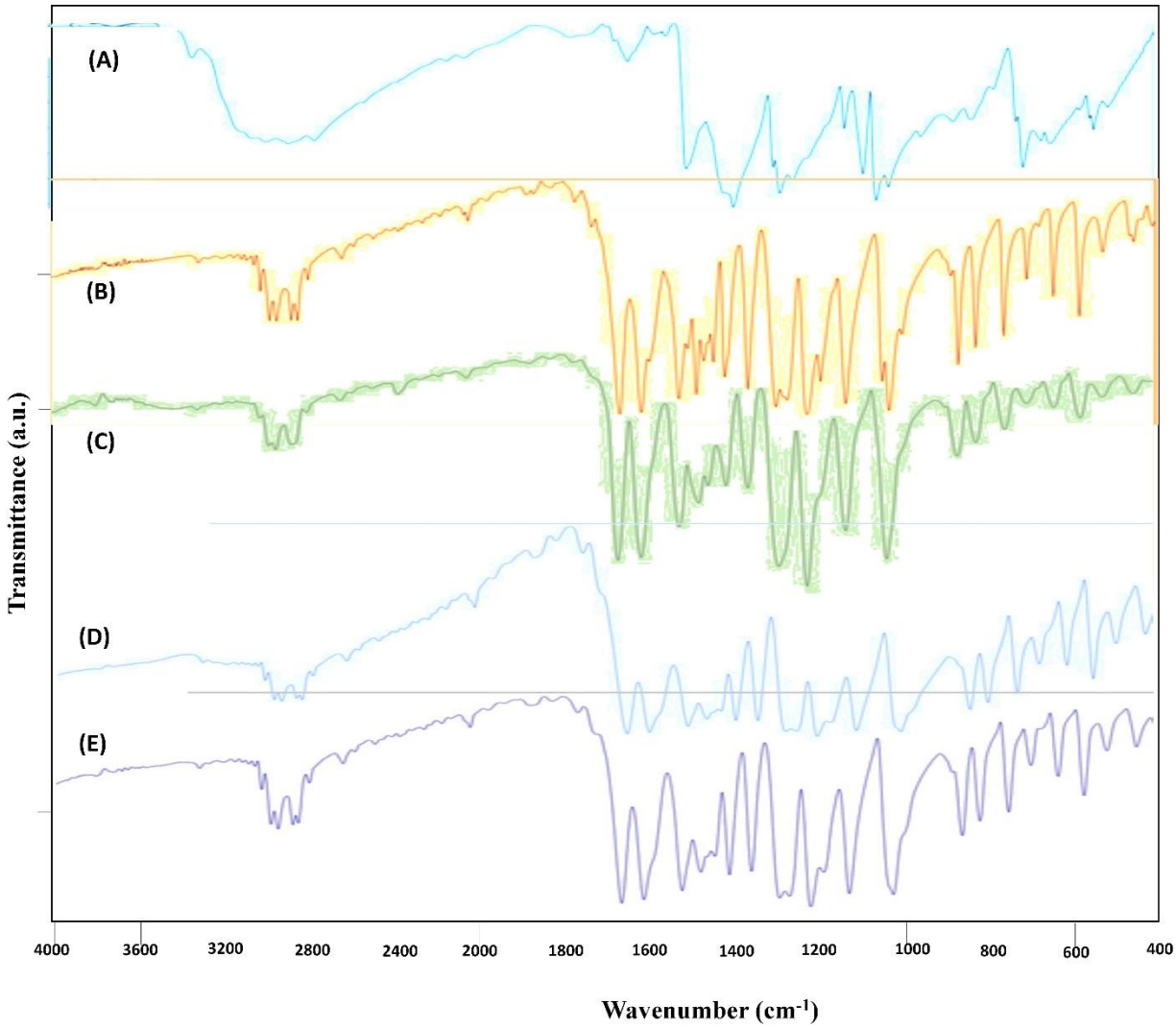

Fig. 5. FT-IR spectra of a) ligand b) Cr-complex c) Fe-complex d) Co-complex e) Cu-complex

After the production and identification of organometallic complexes containing (Cr, Fe, Co, and Cu), firstly, the oxidation of styrene compound using an oxidation agent such as sodium periodate using complex I (Cr-Complex) was chosen as the model reaction for the improvment of the reaction conditions such as solvent, oxidant, type of complex, and catalytic amount (**Table 3**). The pointed reaction was investigated using various solvents, including water, CH_3CN, ethanol, methanol, and different ratio of water and $C_2H_5OH/CH_3OH/CH_3CN$ (**Table 3**, entries 1-10). The obtained yield showed that the mixture of water and ethanol with ration (2:1) was found to be the best solvent for the reaction. Then, the model reaction was investigated using various oxidants, such as sodium periodate, hydrogen peroxide, sodium hypochlorite, and tert-butOOH as oxidants (**Table 3**, entries 11-13). Among the oxidant agents, $NaIO_4$ was chosen as the best oxidant. Also, the amount of organometallic catalyst was investigated, and the 240 mg of complex I (Cr-complex) was obtained as the optimum amount of the organometallic catalyst (**Table 3**, entries 14-16). Moreover, for another catalysts, the optimization reaction conditions were performed (**Table 3**, entries 17-19).

With the optimization reaction condition in hands, the scope and generality of the present approach were checked in the epoxidation of various alkenes (**Table 4**). As shown in **Table 4**, the taget products were produced 72-91% from the epoxidation of various alkenes, including electron-withdrawing (EWG), electron-donating (EDG), and terminal alkenes with long-chain. Other products, such as carboxylic acids, aldehydes, and alcohols, may be produced during epoxidation of alkenes, as has been previously documented in the literature.

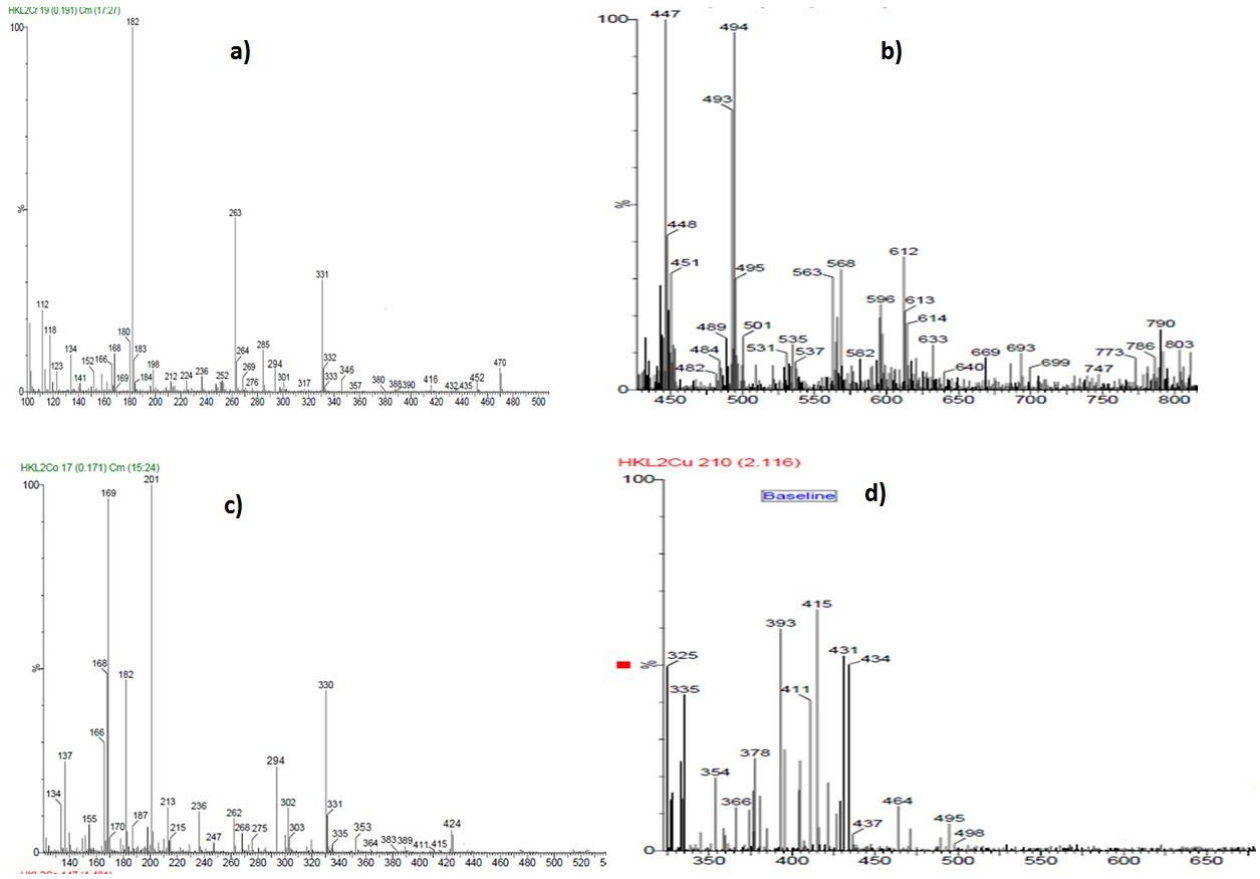

Fig. 6. Mass spectra of a) Cr-complex b) Fe-complex c) Co-complex d) Cu-complex

Table 3. Optimization of reaction conditions for epoxidation of styrene[a]

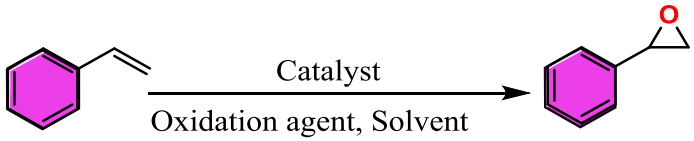

Entry	Oxidant	Solvent	Catalyst	Catalyst amount (mg)	Time (h)	Yield (%)[b]
1	$NaIO_4$	H_2O	Complex I	140	1.5	66
2	$NaIO_4$	CH_3CN	Complex I	140	1.5	62
3	$NaIO_4$	EtOH	Complex I	140	1.5	51
4	$NaIO_4$	MeOH	Complex I	140	1.5	58
5	$NaIO_4$	H_2O/ CH_3CN (1:1)	Complex I	140	1.5	74
6	$NaIO_4$	H_2O/ CH_3CN (2:1)	Complex I	140	1.5	76
7	$NaIO_4$	H_2O/ EtOH (1:1)	Complex I	140	1.5	78
8	$NaIO_4$	H_2O/ EtOH (2:1)	Complex I	140	1.5	80
9	$NaIO_4$	H_2O/ MeOH (1:1)	Complex I	140	1.5	59
10	$NaIO_4$	H_2O/ MeOH (2:1)	Complex I	140	1.5	63
11	H_2O_2	H_2O/ EtOH (2:1)	Complex I	140	1.5	52
12	NaOCl	H_2O/ EtOH (2:1)	Complex I	140	1.5	59

13	tert-ButOOH	H_2O/ EtOH (2:1)	Complex I	140	1.5	56
14	$NaIO_4$	H_2O/ EtOH (2:1)	Complex I	190	1.5	83
15	$NaIO_4$	H_2O/ EtOH (2:1)	Complex I	240	1.5	89
16	$NaIO_4$	H_2O/ EtOH (2:1)	Complex I	300	1.5	86
17	$NaIO_4$	H_2O/ EtOH (2:1)	Complex II	240	1.5	86
18	$NaIO_4$	H_2O/ EtOH (2:1)	Complex III	240	1.5	85
19	$NaIO_4$	H_2O/ EtOH (2:1)	Complex IV	240	1.5	88

a) Reaction conditions: Styrene (2 mmol), oxidant (2 mmol), Solvent (5 mL). Room temperature b) GC Yields based on the starting compound.

Table 4. Epoxidation of alkenes with $NaIO_4$ in the presence of organometallic complexes

Entry	Alkene	Type of complex	Yield (%)[b]	Other products Yield (%)[c]	Time (h)	TOF (h^{-1})
1	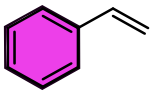	I	89	4	2.5	993
		II	86	6	2.8	857
		III	88	7	3.0	781
		IV	88	8	2.4	1012
2		I	89	8	2.0	1428
		II	87	9	2.2	1223
		III	86	1	1.8	1214
		IV	90	5	2.4	1139
3	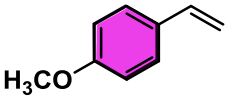	I	90	2	1.8	1317
		II	88	8	1.9	992
		III	89	8	2.0	938
		IV	85	9	2.2	912
4	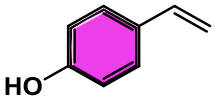	I	83	1	1.8	931
		II	84	5	2.4	878
		III	88	9	3.0	890
		IV	91	3	3.2	837
5	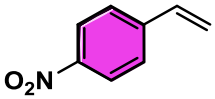	I	88	3	2.7	580
		II	79	9	2.9	566
		III	83	5	3.0	646
		IV	86	3	3.1	686
6	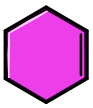	I	83	6	2.5	1270
		II	85	5	2.5	1173
		III	88	3	2.4	1157
		IV	91	4	2.0	964
7	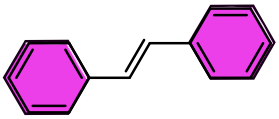	I	79[d]	2	3.4	1217
		II	72[d]	8	3.8	967
		III	75[d]	6	3.4	888
		IV	73[d]	7	3.7	836
8	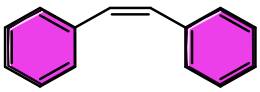	I	84[e]	2	1.8	838
		II	82[e]	6	1.9	952
		III	86[e]	9	2.0	928
		IV	86[e]	16	2.4	987
9	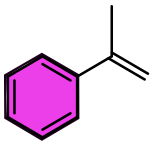	I	83	3	2.2	993
		II	85	9	2.6	847
		III	88	5	2.7	781
		IV	91	3	2.7	1012

10	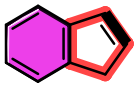	I	83	2	1.8	1438
		II	85	8	1.9	1323
		III	88	6	2.0	1114
		IV	91	7	2.4	1039
11	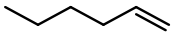	I	86	3	2.2	1317
		II	88	4	2.6	892
		III	84	8	2.7	838
		IV	79	6	2.7	812
12	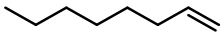	I	88	2	3.0	931
		II	90	9	2.7	878
		III	78	7	2.4	890
		IV	76	6	2.2	892

a) General conditions: Alkene substrate (2.0 mmol), $NaIO_4$ (2.0 mmol), Ambient temperature, Organometallic Catalyst: (240 mg), Solvent: (H_2O: EtOH) (2:1) (5 mL), b) GC yield. c) Other products such as RCHO, ROH, RCOOH. d) Yields refer to Trans product based on ^{1}H NMR spectra. e) Yields refer to cis products.

In order to complete our study, the leaching of metals such as Cr, Fe, Co, and Cu was checked during the recoverability tests. The observation tests revealed that after the fourth catalytic cycle, the level of Cr, Fe, Co, and Cu reduced by only 2.1, 3.5, 5.0, and 4.7 ppm (mg.L^{-1}), respectively, for Complex I, II, III, and IV. These findings demonstrated that Cr, Fe, Co, and Cu organometallic catalysts for the epoxidation of alkenes are effective and valuable (**Table 5**). In addition, after 4th recovery, the prepared catalysts were investigated by FT-IR spectroscopy, and the spectra showed that the functional groups were exist present yet (**Fig. 7**).

Table 5. The reusability of the organometallic catalysts in the epoxidation of styrene. A:(metal leaching) (mg.L^{-1}), B: Yield (%), C: %Recovered catalyst, N.D.: Not Detected)

Run	1st			2nd			3rd			4th		
	A	B	C	A	B	C	A	B	C	A	B	C
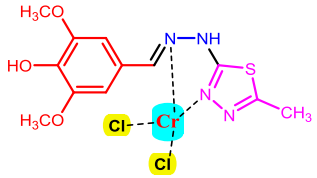	ND, 86%, 99%	1.0, 86%, 99%	ND, 85%, 97%	3.1, 80%, 99%	ND, 86%, 99%	1.0, 86%, 99%	ND, 85%, 97%	3.1, 80%, 99%	ND, 86%, 99%	1.0, 86%, 99%	ND, 85%, 97%	3.1, 80%, 99%
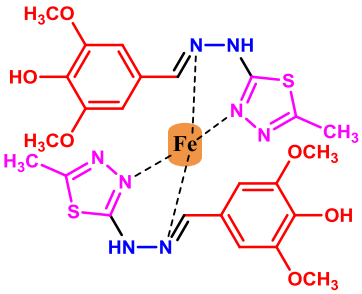	0.6, 83%, 98%	ND, 83%, 99%	ND, 82%, 99%	4.5, 79%, 99%	0.6, 83%, 98%	ND, 83%, 99%	ND, 82%, 99%	4.5, 79%, 99%	0.6, 83%, 98%	ND, 83%, 99%	ND, 82%, 99%	4.5, 79%, 99%

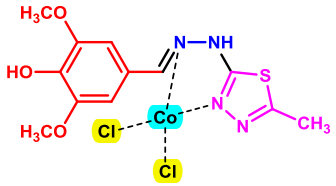	ND, 82%, 99%	ND, 82%, 98%	0.9, 80%, 99%	6.0, 73%, 99%	ND, 82%, 99%	ND, 82%, 98%	0.9, 80%, 99%	6.0, 73%, 99%	ND, 82%, 99%	ND, 82%, 98%	0.9, 80%, 99%	6.0, 73%, 99%
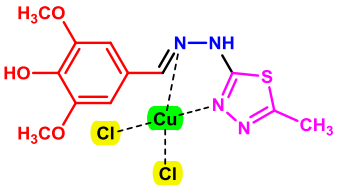	ND, 85%, 99%	0.3, 83%, 97%	ND, 83%, 99%	5.7, 77%, 99%	ND, 85%, 99%	0.3, 83%, 97%	ND, 83%, 99%	5.7, 77%, 99%	ND, 85%, 99%	0.3, 83%, 97%	ND, 83%, 99%	5.7, 77%, 99%

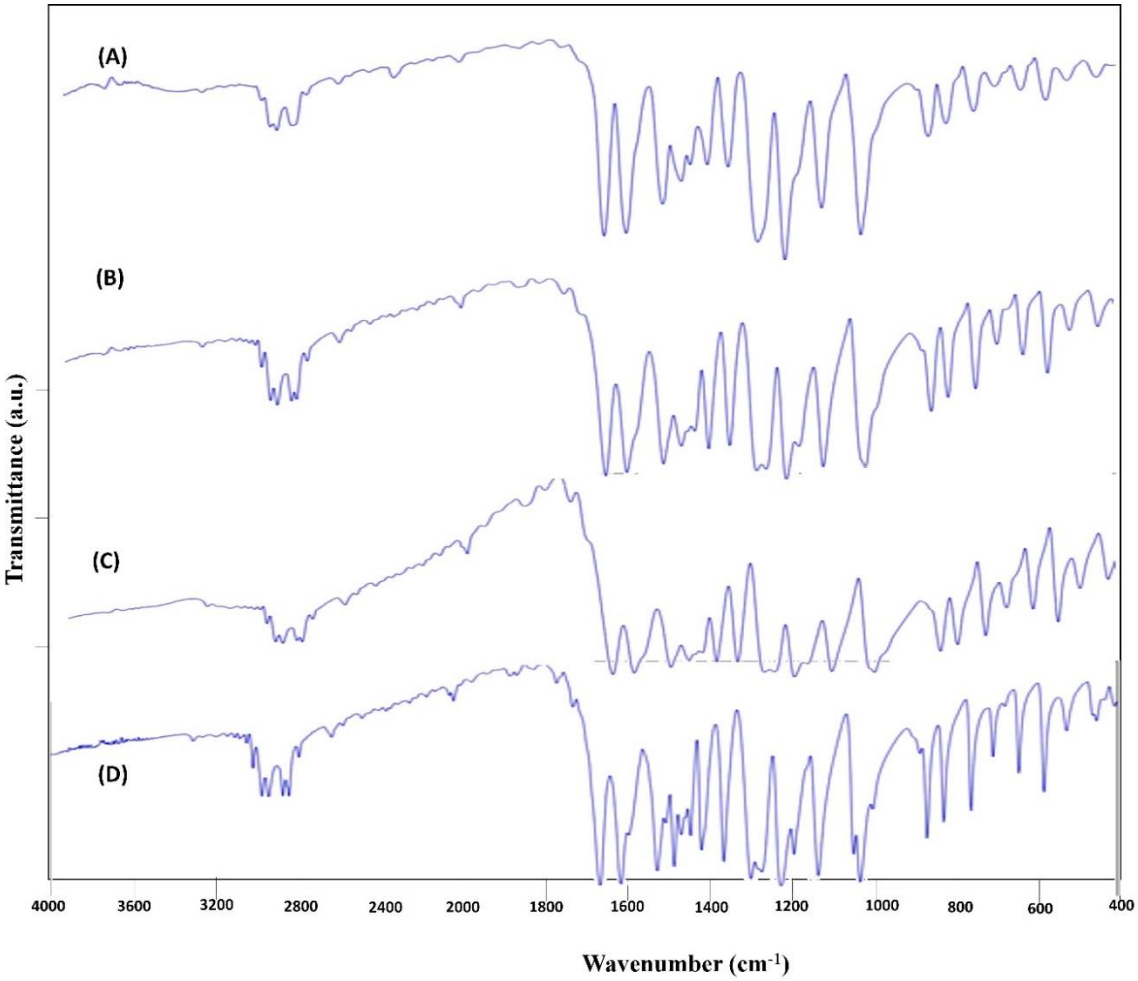

Fig. 7. FT-IR of a) Cr-complex b) Fe-complex c) Co-complex d) Cu-complex after 4th recovery

Using the Agar diffusion technique, the antibacterial activity of 1, 3, and 4-Thiadiazole derivatives was tested against *Staphylococcus aureas* (Gram-positive) and *Escherichia coli* (Gram-negative). Ampicillin was used as a standard drug for testing. Bacterial stock cultures were first revived by inoculating in broth media and growing for 18 hours at 37°C. Wells were formed in the prepared agar plates containing the aforementioned medium. The wells were filled with various amounts of chemicals and antibiotics after 20 minutes. The diameter of the inhibitory zone (mm) on each plate was measured after 24 hours of incubation at 37°C (**Table 6**) (**Fig. 8**).

Table 6. The antibacterial activity of the ligand and organometallic catalysts

Ligand/ Catalyst	*E-coli* Inhibition zone (mm)	*Staph.aurens* Inhibition zone (mm)
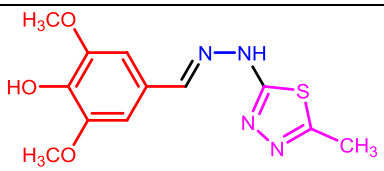	20	15
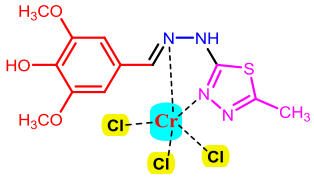	18	17
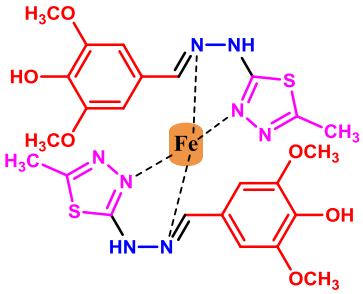	16	15
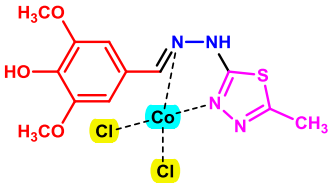	15	18
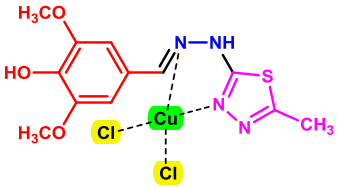	16	14
Ampicillin	20	25

Molecular orbital calculations with DFT for the ligand have been done. The geometry of investigated compound was completely optimized by the DFT method using the 6-311++g(d,p) basis set (**Fig. 9**). The examination of a set of organic molecules using this theoretical model yields excellent results. Without imposing symmetry requirements, all geometries were optimized. Potential surface minima were verified by vibrational frequency calculations. Frontier molecular orbital (FMO) energies were determined in the same way and using the same starting point—the energy gap ($\Delta E = E_{LUMO} - E_{HOMO}$), which separates the energies of the highest occupied molecular orbital (HOMO) and the lowest unoccupied molecular orbital (LUMO). Global reactivity descriptors as the chemical hardness (η), Chemical softness (S), electronegativity (χ), chemical potential (μ), and the electrophilicity index (*w*) of were obtained from the ionization potential (I) and the electron affinity(A) of the ligand following the Koopmans' theorem. All calculations were performed using the Materials studio (2017) software package program (**Tables 7-8**). $I = -E_{HOMO}$ and $A = -E_{LUMO}$, $\eta = (I - A)/2 = (E_{LUMO} - E_{HOMO})/2$, $S = 1/\eta$, $\chi = (I + A)/2$, $\mu = -\chi$, $w = \mu^2/2\eta$

The experimental FTIR spectrum has been recorded in the solid state shown in Figure (6). Theoretically, frequencies are predicted by DFT/B3LYP method using 6-311++G(d,p) basis set presented in **Fig. 10**. The selected experimental and theoretical vibrational frequencies of the ligand with their assignments are listed in **Table 9**. There is a linear correlation between the theoretical data and practical data of vibrational frequencies, and the value of the correlation coefficient equals 0.997, which proves them in agreement.

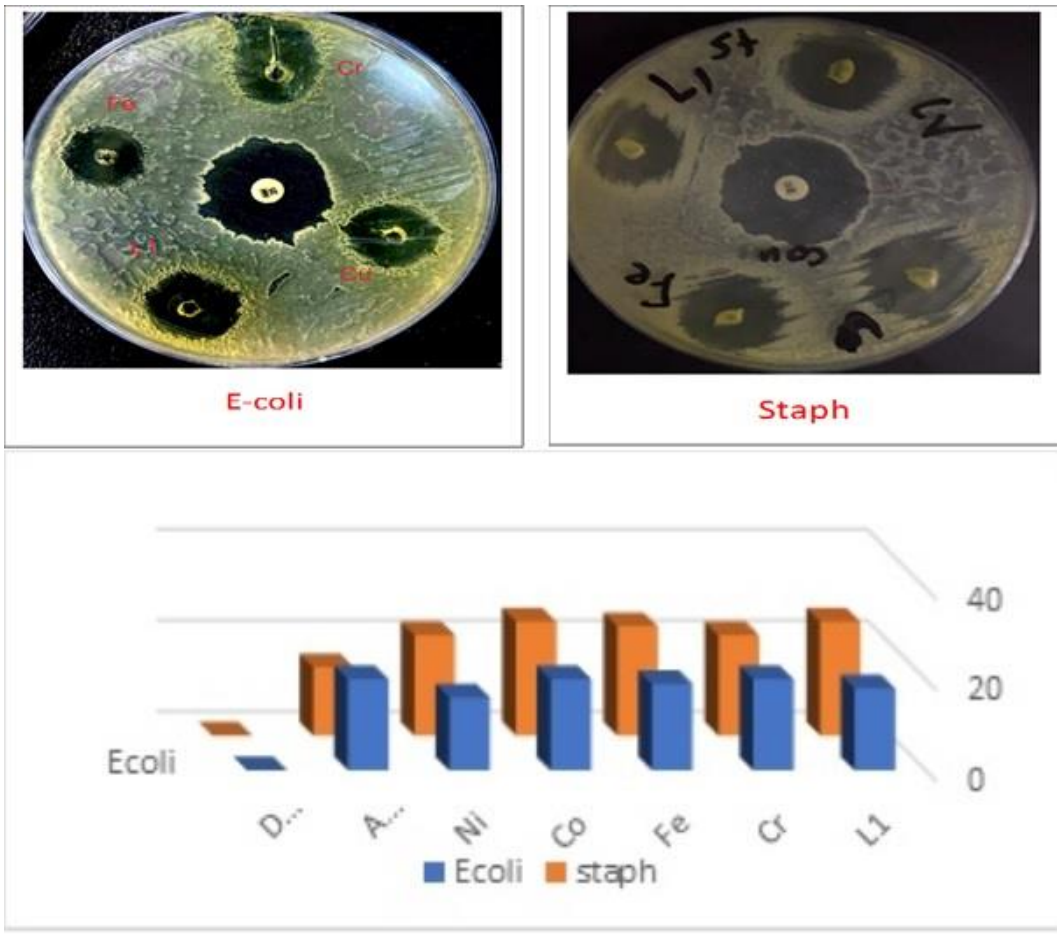

Fig. 8. Diagram activity of the ligand and its complexes against *E-coli* & *Staph.aurens*

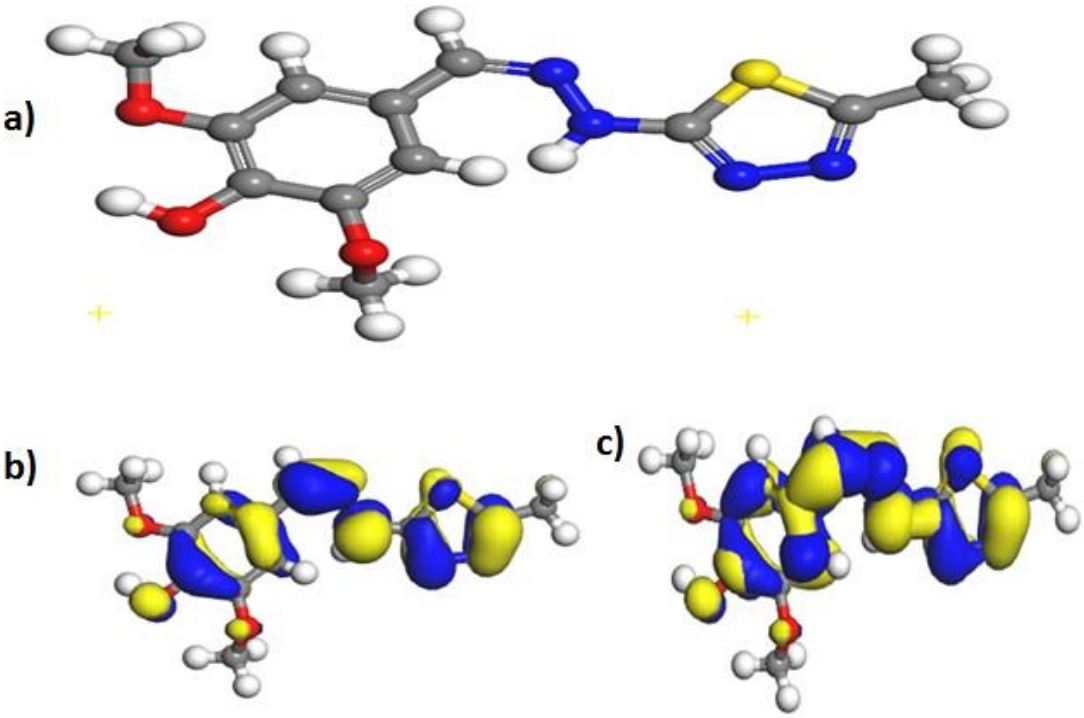

Fig. 9. DFT calculation of ligand a) optimized chemical structure of ligand, b) HOMO of ligand c) LUMO of ligand

Table 7. Electronic parameters

E_{Total} (a.u.)	E_{HOMO} (eV)	E_{LUMO} (eV)	ΔE (eV)	I (eV)	A (eV)
-1299.9044	-4.9738	-2.3054	2.6684	4.9738	2.3054

Table 8. Global reactivity parameters

η (eV)	σ (eV^{-1})	χ (eV)	μ (eV)	ω (eV)	Dipole moment (Debye)
1.3342	0.7495	3.6391	-3.6391	2.3409	6.3802

Table 9. Selected experimental and theoretical vibrational assignments of the ligand

Assignment	Practical frequencies (cm^{-1})	theoretical frequencies (cm^{-1})
O-H str.	3300	3496
N-H str.	3254	3227
C-H aromatic str.	3047	3037
C-H aliphatic str.	2979	2973
C=N imine str.	1660	1654
C=C str.	1608	1634
C=N endo str.	1591	1519
C-S-C str.	1389	1340
N-N str.	1128	1200

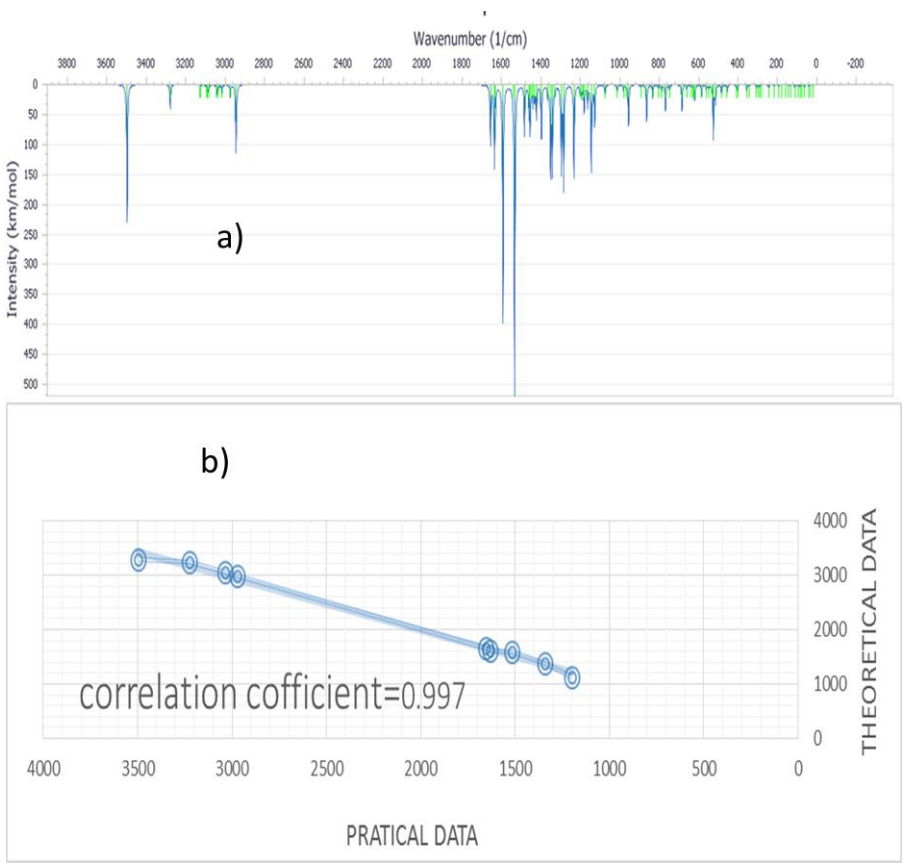

Fig. 10. a) Theoretical IR spectrum of the synthesized ligand, b) Linear correlation between experimental and theoretical frequencies

The geometries of the investigated complexes were fully optimized by using the PM3 method using the hyperchem 8 program (**Fig. 11**). The geometries were in agreement with the experimental result of magnetic susceptibility. In order to show the advantage and efficiency of the present methodology in the epoxidation of alkenes, we have compared the epoxidation of styrene with those of some scientific works in the literature (**Table 10**). The present results reveal that the present new method was worthwhile in terms of catalyst amount, reaction temperature, and time of the reaction, product yield, and reusability of the catalysts.

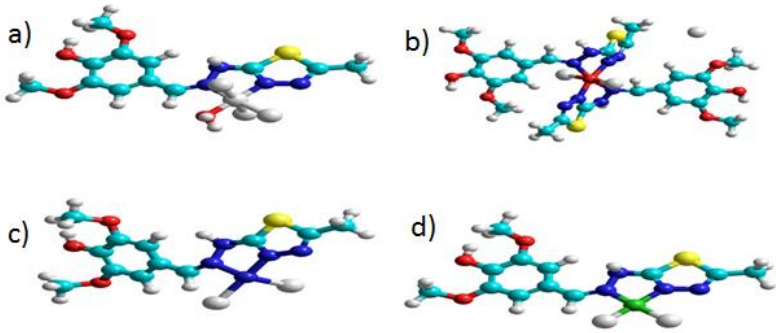

Fig. 11. The DFT calculation of the optimized synthesized complexes

Table 10. Comparison of the results obtained for the epoxidation of styrene

Entry	Catalyst	Catalyst amount	T (°C)	Time	Yield (%)	Ref.
1	Cu/Co-Co PBA-250	12 mol%	250	3 h	89	[36]
2	MnL1-MnL7	8 mol%	100	4 h	90	[43]
3	Vanadium Schiff base	10 mol%	75	4 h	88	[44]
4	$V_2O_5/FeVO_4$	11 mol%	90	2.5 h	87	[45]
5	MCM-41@CP@PAL@Cu	8.5 mol%	100	1.5 h	82	[46]
6	Complex I	5 mol%	RT	2.5	89	This work

In accordance with the previous suggested catalytic cycle of organometallic complex catalyzed epoxidation of alkenes [47], the reaction mechanism pathway for this method is proposed, as illustrated in **Scheme 4**. In the proposed mechanism, the catalyst was activated using $NaIO_4$ in water and ethanol to generate catalyst-oxide (II). In the next step, the catalyst-oxide was reacted with styrene to produce an intermediate (III). Afterward, the intermediate (III) was converted to intermediate (IV), and subsequently styrene oxide was produced, and the catalyst was recovered and moved to the next catalytic cycle.

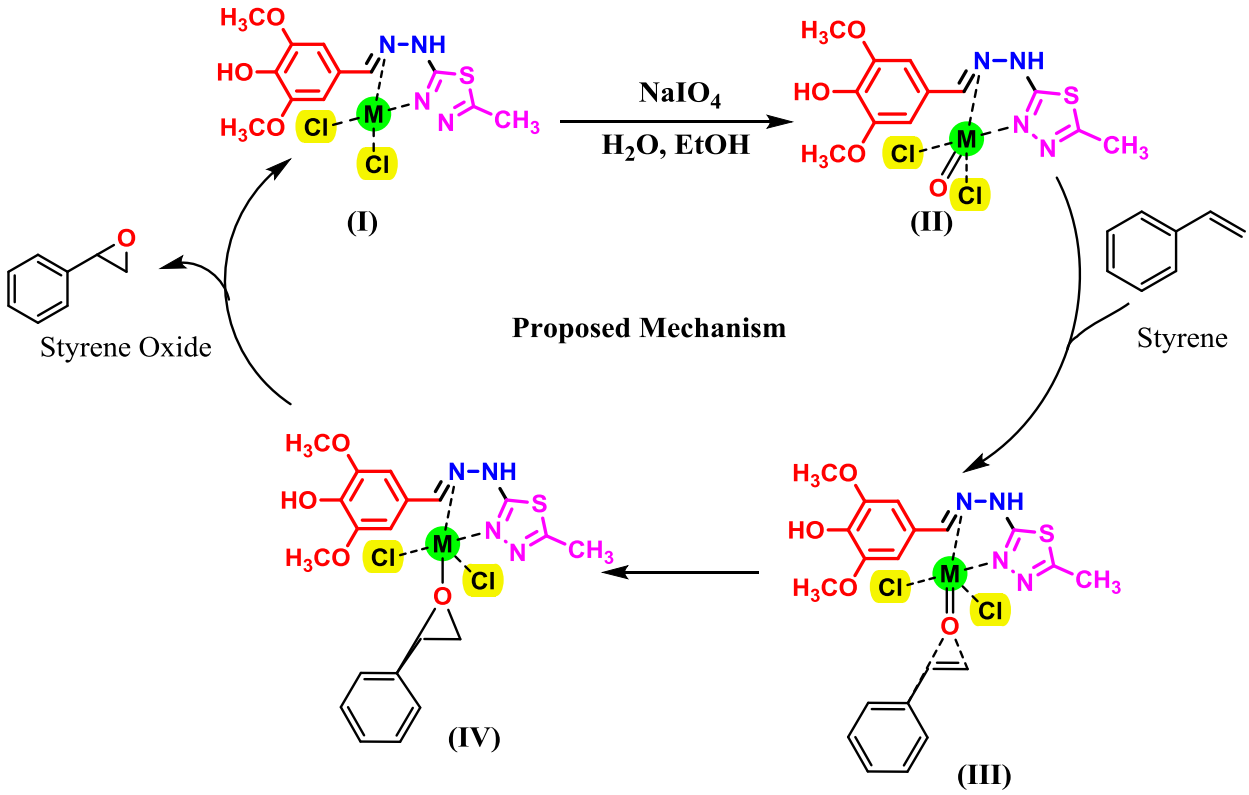

Scheme 4. Proposed reaction pathway for the epoxidation of styrene

4. Conclusions

In summary, the organometallic catalysts were highly efficient and robust organometallic systems for the epoxidation of various alkenes with $NaIO_4$ at ambient temperature. The synthesized catalysts were analyzed by FT-IR spectroscopy, CHN analysis, and magnetic susceptibility. The magnetic momentum of each metal complexes was measured. These magnetic measurements give good idea about the electronic state of the transition metal ion of these complexes. The observed magnetic momentum value of Cr (III) complex was 3.7 BM and 2.9 BM for Fe (III) complex, therefor it is expected octahedral geometry. In addition, the spectra of complexes demonstrated new band vibrational modes for the M-N, and M-Cl group frequencies as a result of bonding the metal ion with the ligand. The produced organometallic catalysts are then utilized in the epoxidation of various alkenes, affording the desired epoxides in good to very good yields. Epoxidation of various alkenes, including electron-withdrawing (EWG), electron-donating (EDG), and long-chain terminal alkenes, yielded 72-91% of the end products. Metal recovery and metal leaching from the produced complexes into the reaction medium were evaluated. Moreover, using the Agar diffusion technique, the antibacterial activity of 1, 3, 4-Thiadiazole derivatives was tested against *Staphylococcus aureas* (Gram-positive) and *Escherichia coli* (Gram-negative). Finally, the geometry of investigated compound was fully optimized by using the DFT method using the 6-311++g(d,p) basis set.

Acknowledgements

We acknowledge the support of this work by the department of chemistry of university of Misan.

Conflicts of interest

The authors declare no conflict of interest.

References

[1] K.C. Gupta, A.K. Sutar, Catalytic activities of Schiff base transition metal complexes, Coord. Chem. Rev., 252 (2008) 1420-1450.

[2] K. Kar, D. Ghosh, B. Kabi, A. Chandra, A concise review on cobalt Schiff base complexes as anticancer agents, Polyhedron, (2022) 115890.

[3] H. Kargar, M. Fallah-Mehrjardi, R. Behjatmanesh-Ardakani, H.A. Rudbari, A.A. Ardakani, S. Sedighi-Khavidak, K.S. Munawar, M. Ashfaq, M.N. Tahir, Synthesis, spectral characterization, crystal structures, biological activities, theoretical calculations and substitution effect of salicylidene ligand on the nature of mono and dinuclear Zn (II) Schiff base complexes, Polyhedron, 213 (2022) 115636.

[4] A.S. Al-Wasidi, I.I.S. AlZahrani, H.I. Thawibaraka, A.M. Naglah, Facile synthesis of ZnO and Co3O4 nanoparticles by thermal decomposition of novel Schiff base complexes: Studying biological and catalytic properties, Arabian Journal of Chemistry, 15 (2022) 103628.

[5] A. Kumar, V. Bhakuni, Enantioselective epoxidation using liposomised m-chloro-perbenzoic acid (LIP MCPBA), Tetrahedron Lett., 37 (1996) 4751-4754.

[6] D.N. Platonov, G.P. Okonnishnikova, R.A. Novikov, K.Y. Suponitsky, Y.V. Tomilov, A novel and unusual reaction of 1,2,3,4,5,6,7-hepta(methoxycarbonyl)-cyclohepta-2,4,6-trien-1-yl potassium with organic azides, Tetrahedron Lett., 55 (2014) 2381-2384.

[7] T. Maharana, N. Nath, H.C. Pradhan, S. Mantri, A. Routaray, A.K. Sutar, Polymer-supported first-row transition metal schiff base complexes: Efficient catalysts for epoxidation of alkenes, React. Funct. Polym., 171 (2022) 105142.

[8] M. Samani, M.H. Ardakani, M. Sabet, Efficient and selective oxidation of hydrocarbons with tert-butyl hydroperoxide catalyzed by oxidovanadium(IV) unsymmetrical Schiff base complex supported on γ-Fe2O3 magnetic nanoparticles, Res. Chem. Intermed., 48 (2022) 1481-1494.

[9] J. Rakhtshah, A comprehensive review on the synthesis, characterization, and catalytic application of transition-metal Schiff-base complexes immobilized on magnetic Fe3O4 nanoparticles, Coord. Chem. Rev., 467 (2022) 214614.

[10] M. Payam, H. Kargar, M. Fallah-Mehrjardi, Silica-coated nanomagnetite-supported oxovanadium(V) Schiff base complex: Preparation, characterization, and catalytic application for the oxidation of sulfides, Inorg. Chem. Commun., 145 (2022) 109951.

[11] M. Bashir, M. Saifullah, M. Riaz, M. Arshad, A. Irfan, S. Iqbal, Z.H. Farooqi, R. Begum, Schiff bases derived from phloroglucinol carbonyl variants and their applications-A review, Inorg. Chem. Commun., 152 (2023) 110690.

[12] H. Kargar, M. Moghadam, L. Shariati, N. Feizi, M. Fallah-Mehrjardi, R. Behjatmanesh-Ardakani, K.S. Munawar, Synthesis, crystal structure, spectral characterization, theoretical studies, and investigation of catalytic activity in selective oxidation of sulfides by

oxo-peroxo tungsten(VI) Schiff base complex, J. Mol. Struct., 1257 (2022) 132608.

[13] C. Boulechfar, H. Ferkous, A. Delimi, A. Djedouani, A. Kahlouche, A. Boublia, A.S. Darwish, T. Lemaoui, R. Verma, Y. Benguerba, Schiff bases and their metal complexes: a review on the history, synthesis, and applications, Inorg. Chem. Commun., (2023) 110451.

[14] T. Ashraf, B. Ali, H. Qayyum, M.S. Haroone, G. Shabbir, Pharmacological aspects of schiff base metal complexes: A critical review, Inorg. Chem. Commun., (2023) 110449.

[15] M. Zabiszak, J. Frymark, K. Ogawa, M. Skrobańska, M. Nowak, R. Jastrzab, M.T. Kaczmarek, Complexes of β-lactam antibiotics and their Schiff-base derivatives as a weapon in the fight against bacterial resistance, Coord. Chem. Rev., 493 (2023) 215326.

[16] K. Mondal, S. Mistri, Schiff base based metal complexes: A review of their catalytic activity on aldol and henry reaction, Comments Inorg. Chem., 43 (2023) 77-105.

[17] L.H. Abdel-Rahman, A.A. Abdelghani, A.A. AlObaid, D.A. El-ezz, I. Warad, M.R. Shehata, E.M. Abdalla, Novel Bromo and methoxy substituted Schiff base complexes of Mn (II), Fe (III), and Cr (III) for anticancer, antimicrobial, docking, and ADMET studies, Sci. Rep., 13 (2023) 3199.

[18] Y.-L. Dong, H.-R. Liu, S.-M. Wang, G.-W. Guan, Q.-Y. Yang, Immobilizing Isatin-Schiff Base Complexes in NH2-UiO-66 for Highly Photocatalytic CO2 Reduction, ACS Catal., 13 (2023) 2547-2554.

[19] C. Gautam, D. Srivastava, G. Kociok-Köhn, S.W. Gosavi, V.K. Sharma, R. Chauhan, D.J. Late, A. Kumar, M. Muddassir, Copper (ii) and cobalt (iii) Schiff base complexes with hydroxy anchors as sensitizers in dye-sensitized solar cells (DSSCs), RSC Adv., 13 (2023) 9046-9054.

[20] A.S. Mohammed, J.M. Alyass, K.I. Khallow, Synthesis and Characterization of Hybrid Dual Metallic Complexes of Schiff Base Containing (Cd and Mn/Fe/Co/Ni) Derived from Isatin and 1,4-Phenylenediamine As Novel Organometallic Catalysts for Rapid and Efficient Epoxidation of Alkenes, Iran. J. Catal., 12 (2022) 223-235.

[21] H. Zakeri, S. Rayati, G. Zarei, A. Parsa, F. Adhami, Mn(II)-Schiff base complex immobilized onto MCM-41 matrix as a heterogeneous catalyst for epoxidation of alkenes, Iran. J. Catal., 10 (2020) 71-78.

[22] M. Tayebani, B. Shafaat, M. Iravani, Hydrogen peroxide oxidation of primary alcohols by thiosemicarbazide Schiff base metal complexes, Iran. J. Catal., 5 (2015) 213-221.

[23] I.R. Parrey, A.A. Hashmi, B.L. Swami, S.A. AL-Thabaiti, Synthesis, characterisation and catalytic activity of Schiff base Cu(II) metal complex, Iran. J. Catal., 5 (2015) 89-95.

[24] M.K. Chug, E.J. Brisbois, Recent Developments in Multifunctional Antimicrobial Surfaces and Applications toward Advanced Nitric Oxide-Based Biomaterials, ACS Materials Au, 2 (2022) 525-551.

[25] Q. Xu, K.-S. Huang, Y.-F. Wang, H.-H. Wang, B.-D. Cui, W.-Y. Han, Y.-Z. Chen, N.-W. Wan, Stereodivergent Synthesis of Epoxides and Oxazolidinones via the Halohydrin Dehalogenase-Catalyzed Desymmetrization Strategy, ACS Catal., 12 (2022) 6285-6293.

[26] R. Ma, X. Hua, C.-L. He, H.-H. Wang, Z.-X. Wang, B.-D. Cui, W.-Y. Han, Y.-Z. Chen, N.-W. Wan, Biocatalytic Thionation of Epoxides for Enantioselective Synthesis of Thiiranes, Angew. Chem. Int. Ed., 61 (2022) e202212589.

[27] G. An, C.a. Wang, H. Gao, G. Wang, Y. Luo, Z. Liu, C. Xia, S. Liu, X. Peng, Z. Cheng, X. Shu, A novel MOFs-induced strategy for preparing anatase-free hierarchical TS-1 zeolite:synthesis routes, growth mechanisms and enhanced catalytic performance, J. Colloid Interface Sci., 633 (2023) 291-302.

[28] S. Singh, D.B. Singh, B. Gautam, A. Singh, N. Yadav, Chapter 19 - Pharmacokinetics and pharmacodynamics analysis of drug candidates, in: D.B. Singh, R.K. Pathak (Eds.) Bioinformatics, Academic Press2022, pp. 305-316.

[29] M.S.S. Adam, S. Shaaban, N.M. El-Metwaly, Two ionic oxo-vanadate and dioxo-molybdate complexes of dinitro-aroylhydrazone derivative: Effective catalysts for epoxidation reactions, biological activity, ctDNA binding, density functional theory, and in silico investigations, Appl. Organomet. Chem., 36 (2022) e6763.

[30] B.N. Patra, P. Ghosh, N. Sepay, S. Gayen, S. Koner, P. Brandao, Z. Lin, R. Debnath, J.L. Pratihar, T. Maity, D. Mal, Aerobic epoxidation of olefins by carboxylate ligand-based cobalt (II) compound: synthesis, X-ray crystallography, and catalytic exploration, Appl. Organomet. Chem., 36 (2022) e6552.

[31] S. Verma, A. Joshi, S.R. De, J.L. Jat, Methyltrioxorhenium (MTO) catalysis in the

epoxidation of alkenes: a synthetic overview, New J. Chem., 46 (2022) 2005-2027.

[32] M. Li, L. Ma, L. Luo, Y. Liu, M. Xu, H. Zhou, Y. Wang, Z. Li, X. Kong, H. Duan, Efficient photocatalytic epoxidation of styrene over a quantum-sized SnO2 on carbon nitride as a heterostructured catalyst, Applied Catalysis B: Environmental, 309 (2022) 121268.

[33] Y. Wu, Z. Chen, Y. Wang, J. Xu, Kinetic Studies and Reaction Network in the Epoxidation of Styrene Catalyzed by the Temperature-Controlled Phase-Transfer Catalyst [(C18H37)2(CH3)2N]7[PW11O39], Indust. Eng. Chem. Res., 61 (2022) 10747-10755.

[34] R.A. Bepari, P. Bharali, B.K. Das, Synthesis of nanoscale CuO via precursor method and its application in the catalytic epoxidation of styrene, RSC Adv., 12 (2022) 6044-6053.

[35] S. Chatterjee, S. Das, P. Bhanja, E. E. S, R. Thapa, S. Ruidas, S. Chongdar, S. Ray, A. Bhaumik, Ag nanoparticles immobilized over highly porous crystalline organosilica for epoxidation of styrene using CO2 as oxidant, Journal of CO2 Utilization, 55 (2022) 101843.

[36] Y. Fu, L. Liu, S. Tricard, K. Liang, J. Zhang, J. Fang, J. Zhao, Slow pyrolysis of Cu/Co-Co Prussian blue analog to enhance catalytic activity and selectivity in epoxidation of styrene, Appl. Catal., A, 657 (2023) 119161.

[37] Y. Zhang, A. Iqbal, J. Zai, S.-Y. Zhang, H. Guo, X. Liu, I. ul Islam, H. Fazal, X. Qian, Bromine and oxygen redox species mediated highly selective electro-epoxidation of styrene, Organic Chemistry Frontiers, 9 (2022) 436-444.

[38] Y. Zhang, A. Iqbal, J. Zai, W. Li, H. Guo, X. Meng, W. Li, I.u. Islam, Z. Xin, X. Qian, Balanced cathodic debromination and hydrogen evolution reactions endow highly selective epoxidation of styrene, Composites Part B: Engineering, 246 (2022) 110281.

[39] Z. Zhang, J. Tang, J. Chen, P. Cui, S. Jiao, W. Yi, Q. Ke, H. Yang, Efficient epoxidation of styrene within pickering emulsion-based compartmentalized microreactors, Catal. Today, 410 (2023) 222-230.

[40] W. Emori, G.J. Ogunwale, H. Louis, E.C. Agwamba, K. Wei, T.O. Unimuke, C.-R. Cheng, E.U. Ejiofor, F.C. Asogwa, A.S. Adeyinka, Spectroscopic (UV–vis, FT-IR, FT-Raman, and NMR) analysis, structural benchmarking, molecular properties, and the in-silico cerebral anti-ischemic activity of 2-amino-6-ethoxybenzothiazole, J. Mol. Struct., 1265 (2022) 133318.

[41] P.V. Ramana, Y.R. Krishna, K.C. Mouli, Experimental FT-IR and UV–Vis spectroscopic studies and molecular docking analysis of anti-cancer drugs Exemestane and Pazopanib, J. Mol. Struct., 1263 (2022) 133051.

[42] S. Janeoo, Reenu, A. Saroa, R. Kumar, H. Kaur, Computational investigation of bioactive 2,3-diaryl quinolines using DFT method: FT- IR, NMR spectra, NBO, NLO, HOMO-LUMO transitions, and quantum-chemical properties, J. Mol. Struct., 1253 (2022) 132285.

[43] B. Maleki, R. Sandaroos, S. Peiman, Mn (III) Schiff base complexes containing crown ether rings immobilized onto MCM-41 matrix as heterogeneous catalysts for oxidation of alkenes, Heliyon, 9 (2023).

[44] C.A. Salubi, Heterogeneous vanadium Schiff base complexes in catalytic oxidation reactions, UWC Scholar Publication, 2023 (2023) 110-119.

[45] J. Liu, W. Wang, L. Wang, P. Jian, Heterostructured V2O5/FeVO4 for enhanced liquid-phase epoxidation of cyclooctene, J. Colloid Interface Sci., 630 (2023) 804-812.

[46] A. Malik, U.P. Singh, Functionalized MCM-41 based recyclable catalyst (MCM-41@CP@PAL@Cu) for the epoxidation of alkenes using tert-BuOOH, J. Porous Mater., (2023) 2012-2019.

[47] M. Abboud, N. Al-Zaqri, T. Sahlabji, M. Eissa, A.T. Mubarak, R. Bel-Hadj-Tahar, A. Alsalme, F.A. Alharthi, A. Alsyahi, M.S. Hamdy, Instant and quantitative epoxidation of styrene under ambient conditions over a nickel(ii)dibenzotetramethyltetraaza[14]annulene complex immobilized on amino-functionalized SBA-15, RSC Adv., 10 (2020) 35407-35418.